Polar Compounds Constructed with the $[Cr_2O_7]^{2-}$ Anion

Alexander J. Norquist,[†] Kevin R. Heier,[‡] P. Shiv Halasyamani,[§] Charlotte L. Stern, and Kenneth R. Poeppelmeier*

Department of Chemistry, Northwestern University, Evanston, Illinois 60208-3113

Received August 18, 2000

Crystalline $KTiOPO_4$ (KTP), an inorganic nonlinear optical material with a waveguide figure-of-merit that is twice that of other mixed-metal oxides, contains helical chains of $TiO_{4/2}O_{2/2}$ octahedra in which a long, short Ti−O bond motif results in a net *c*-directed polarization. The alternating long and short Ti−O bonds that occur along these chains are the major contributors to the large nonlinear optic and electrooptic coefficients. Analogous chains have been constructed using dichromate $[Cr_2O_7]^{2-}$anions and $[M(py)_4]^{2+}$ (M = Cu, Zn) cations; these new transition metal oxides crystallize in the same space group as KTP. Crystal data for $Cu(py)_4Cr_2O_7$: orthorhombic, space group $Pna2_1$ (No. 33), with $a = 15.941(7)$ Å, $b = 16.324(3)$ Å, $c = 8.857(2)$ Å, and $Z = 4$; for $Zn(py)_4Cr_2O_7$, orthorhombic, space group $Pna2_1$ (No. 33), with $a = 16.503(1)$ Å, $b = 16.005(1)$ Å, $c = 8.8130(5)$ Å, and $Z = 4$; for $Cd(py)_4Cr_2O_7$, monoclinic, space group $C2/c$ (No. 15), with $a = 14.8034(9)$ Å, $b = 11.1847(7)$ Å, $c = 15.788(1)$ Å, $\beta = 110.023(1)°$, and $Z = 4$.

Introduction

Inherently acentric molecules can provide building blocks for the synthesis of new framework materials with possible ferroelectric and second-order nonlinear optical (NLO) behavior. The acentric oxide fluorides $[NbOF_5]^{2-}$,[1−4] $[TaOF_5]^{2-}$,[4] $[WO_2F_4]^{2-}$,[5,6] and $[MoO_2F_4]^{2-}$ [3] have been crystallized into a host of new mixed-metal materials that combine the octahedral and dinegative oxide fluoride anions with dipositive cations, typically $[Cu(py)_4]^{2+}$. In the primary $[MX_6]^{2-}$ (MX_6 = $NbOF_5$, $TaOF_5$, MoO_2F_4, and WO_2F_4) units, the displacement of the transition metal produces a noncentrosymmetric environment as well as a local polarization. The intraoctahedral distortions observed in the primary $[MX_6]^{2-}$ units, and in $KTiOPO_4$,[7] $LiNbO_3$,[8] and other traditional materials, are compatible with the polar crystal classes 4mm(C_{4v}), 3m(C_{3v}), or mm2(C_{2v}), in which both ferroelectric and second-order NLO behavior are possible.

The $[MO_4]^{n-}$ tetrahedron is another acentric building block that can be used to create noncentrosymmetric materials. For example, potassium dihydrogen phosphate is a ferroelectric material with discreet PO_4 tetrahedra.[9] The dichromate ion, $[Cr_2O_7]^{2-}$, is another attractive candidate for study. The syntheses, structures, second harmonic signals, and infrared spectra of $Cu(py)_4Cr_2O_7$, $Zn(py)_4Cr_2O_7$, and $Cd(py)_4Cr_2O_7$ are reported in this paper. The combination of an octahedral cation with the dichromate anion results in $M(py)_4Cr_2O_7$ (M = Cu, Zn) chains similar to the $TiO_{4/2}O_{2/2}$ helices in $KTiOPO_4$ (KTP).[7] In KTP the short "titanyl" and long Ti−O bonds within each helical chain facilitate the large NLO response.[10−13]

Experimental Section

CAUTION. $(HF)_x$·pyridine is toxic and corrosive!

Materials. CuO (99.99% Aldrich), ZnO (99.99% Aldrich), CdO (99.5% Aldrich), $[pyH]_2[Cr_2O_7]$ (pyridinium dichromate, 98% Aldrich), pyridine (99.9% anhydrous, Aldrich), and $(HF)_x$·pyridine (pyridinium poly(hydrogen fluoride), 70% HF by weight, Aldrich) were used as received. Reagent amounts of deionized H_2O were also used in the synthesis.

Synthesis. Single crystals of each of the reported compounds were synthesized by placing the appropriate amounts of reactants (see below) in Teflon (fluoro-ethylene-propylene) "pouches".[14] The pouches were sealed and placed in a 2000 mL autoclave filled with 600 mL of water. The autoclave was heated for 24 h at 150 °C and cooled to room temperature over an additional 24 h. The pouches were opened in air, and products were recovered by filtration.

$Cu(py)_4Cr_2O_7$. The compound $Cu(py)_4Cr_2O_7$ was synthesized by adding 3.95×10^{-2} g (4.97×10^{-4} mol) of CuO and 1.005×10^{-1} g (2.67×10^{-4} mol) of $[pyH]_2[Cr_2O_7]$ to a Teflon pouch. To this mixture were added 2.067×10^{-1} g (7.85×10^{-4} mol) of $(HF)_x$·pyridine, 5.89×10^{-2} g (3.27×10^{-3} mol) of H_2O, and 1.4937 g (1.89×10^{-2} mol) of pyridine. Green-yellow crystals were recovered in 60% yield based on copper.

* Corresponding author.

† Present address: Inorganic Chemistry Laboratory, Oxford University, Oxford OX1 3QR, U.K.

‡ Present address: Air Products and Chemicals, Inc., Allentown, PA 18195.

§ Present address: Department of Chemistry, University of Houston, Houston, TX 77204-5641.

(1) Halasyamani, P.; Willis, M. J.; Stern, C. L.; Lundquist, P. M.; Wong, G. K.; Poeppelmeier, K. R. *Inorg. Chem.* **1996**, *35*, 1367.
(2) Halasyamani, P.; Heier, K. R.; Willis, M. J.; Stern, C. L.; Poeppelmeier, K. R. *Z. Anorg. Allg. Chem.* **1996**, *622*, 479.
(3) Heier, K. R.; Norquist, A. J.; Wilson, C. G.; Stern, C. L.; Poeppelmeier, K. R. *Inorg. Chem.* **1998**, *37*, 76.
(4) Norquist, A. J.; Stern, C. L.; Poeppelmeier, K. R. *Inorg. Chem.* **1999**, *38*, 3448.
(5) Halasyamani, S.; Heier, K. R.; Stern, C. L.; Poeppelmeier, K. R. *Acta Crystallogr., Sect. C* **1997**, *53*, 1240.
(6) Heier, K. R.; Norquist, A. J.; Halasyamani, P. S.; Duarte, A.; Stern, C. L.; Poeppelmeier, K. R. *Inorg. Chem.* **1999**, *38*, 762.
(7) Trodjman, I. Masse, R.; Guitel, J. C. *Z. Kristallogr.* **1974**, *139*, 103.
(8) Mattias, B. T.; Remeika, J. P. *Phys. Rev.* **1949**, *76*, 1886.
(9) Peterson, S. W.; Levy, H. A.; Simonsen, S. H. *Phys. Rev.* **1954**, *93*, 1120.
(10) Stucky, G. D.; Phillips, M. L. F.; Gier, T. E. *Chem. Mater.* **1989**, *1*, 492.
(11) Phillips, M. L. F.; Harrison, W. T. A.; Gier, T. E.; Stucky, G. D.; Kulkarni, G. V.; Burdett, J. K. *Inorg. Chem.* **1990**, *29*, 2158.
(12) Munowitz, M.; Jarman, R. H.; Harrison, J. F. *Chem. Mater.* **1993**, *5*, 661.
(13) Hagerman, M. E.; Poeppelmeier, K. R. *Chem. Mater.* **1995**, *7*, 602.
(14) Harrison, W. T. A.; Nenoff, T. M.; Gier, T. E.; Stucky, G. D. *Inorg. Chem.* **1993**, *32*, 2437.

10.1021/ic000953y CCC: $20.00
Published on Web 03/16/2001

Table 1. Crystallographic Data for $M(py)_4Cr_2O_7$ (M = Cu, Zn, Cd)

data	$Cu(py)_4Cr_2O_7$	$Zn(py)_4Cr_2O_7$	$Cd(py)_4Cr_2O_7$
formula	$CuCr_2C_{20}H_{20}N_4O_7$	$ZnCr_2C_{20}H_{20}N_4O_7$	$CdCr_2C_{20}H_{20}N_4O_7$
a (Å)	15.927(2)	16.503(1)	14.8034(9)
b (Å)	16.311(2)	16.005(1)	11.1847(7)
c (Å)	8.8513(9)	8.8130(5)	15.788(1)
β (deg)			110.023(1)
V (Å^3)	2299.4(3)	2327.8(2)	2456.0(2)
Z	4	4	4
fw	595.94	597.77	644.80
space group	$Pna2_1$ (No. 33)	$Pna2_1$ (No. 33)	$C2/c$ (No. 15)
T (°C)	−120(1)	−120(1)	−120(1)
λ (Å)	0.71069	0.71069	0.71069
ρ_{calcd} (g/cm^3)	1.721	1.706	1.744
ρ_{obsd} (g/cm^3)[a]	1.70(5)	1.680(3)	1.661(3)
μ (cm^{-1})	18.95	19.89	17.75
$R(F)$[b]	0.032	0.039	0.032
$R_w(F)$[c]	0.034	0.032	0.029

[a] Density measured by flotation pycnometry at 24 °C. [b] $R = \sum||F_o| - |F_c||/\sum|F_o|$. [c] $R_w = [\sum(|F_o| - |F_c|)^2/\sum(F_o)^2]^{1/2}$.

Table 2. Selected Atomic Coordinates for $Cu(py)_4Cr_2O_7$

atom	site	x	y	z	B_{eq}[a]	occ
Cu	4a	0.20527(1)	0.74747(1)	0.7727	1.712(5)	1
Cr(1)	4a	0.19674(2)	0.56571(2)	0.48907(5)	2.533(8)	1
Cr(2)	4a	0.29195(2)	0.40279(2)	0.60811(4)	2.186(8)	1
O(1)	4a	0.21388(9)	0.64557(8)	0.5944(2)	2.98(4)	1
O(2)	4a	0.1011(1)	0.5659(1)	0.4345(2)	6.11(6)	1
O(3)	4a	0.2591(1)	0.5638(1)	0.3498(2)	6.90(7)	1
O(4)	4a	0.20914(8)	0.47558(8)	0.6036(2)	3.38(4)	1
O(5)	4a	0.38181(9)	0.4455(1)	0.6342(2)	4.04(5)	1
O(6)	4a	0.29306(9)	0.35040(8)	0.4536(2)	2.74(4)	1
O(7)	4a	0.27219(9)	0.34131(9)	0.7466(2)	3.77(5)	1
N(1)	4a	0.2946(1)	0.68427(9)	0.8896(2)	1.939(4)	1
N(2)	4a	0.1132(1)	0.8083(1)	0.6605(2)	1.94(4)	1
N(3)	4a	0.1158(1)	0.68611(9)	0.8904(2)	1.81(4)	1
N(4)	4a	0.2911(1)	0.81288(9)	0.6545(2)	1.75(4)	1

[a] $B_{eq} = (8/3)\pi^2U_{11}(aa^*)^2 + U_{22}(bb^*)^2 + U_{33}(cc^*)^2 + 2U_{12}(aa^*bb^*)\cos\gamma + 2U_{13}(aa^*cc^*)\cos\beta + 2U_{23}(bb^*cc^*)\cos\alpha$.

$Zn(py)_4Cr_2O_7$. The compound $Zn(py)_4Cr_2O_7$ was synthesized by adding 5.28×10^{-2} g (6.57×10^{-4} mol) of ZnO and 1.04×10^{-1} g (2.76×10^{-4} mol) of $[pyH]_2[Cr_2O_7]$ to a Teflon pouch. To this mixture were added 1.91×10^{-1} g (7.23×10^{-4} mol) of $(HF)_x$·pyridine, 7.25×10^{-2} g (4.03×10^{-3} mol) of H_2O, and 1.578 g (1.997×10^{-2} mol) of pyridine. Orange crystals were recovered in 50% yield based on zinc.

$Cd(py)_4Cr_2O_7$. The compound $Cd(py)_4Cr_2O_7$ was synthesized by adding 4.45×10^{-2} g (3.47×10^{-4} mol) of CdO and 1.005×10^{-1} g (2.67×10^{-4} mol) of $[pyH]_2[Cr_2O_7]$ to a Teflon "pouch". To this mixture were added 1.76×10^{-1} g (6.67×10^{-4} mol) of $(HF)_x$·pyridine, 5.21×10^{-2} g (2.89×10^{-3} mol) of H_2O, and 1.503 g (1.902×10^{-2} mol) of pyridine. Orange crystals were recovered in 60% yield based on cadmium.

Crystallographic Determination. Relevant crystallographic data are listed in Table 1. All calculations were performed using the TEXSAN crystallographic software package from Molecular Structure Corporation.[15] The structures were solved by direct methods[16] and expanded using Fourier techniques.[17] Detailed crystallographic information for all three structures is available in the Supporting Information in CIF format.

$Cu(py)_4Cr_2O_7$. Based on systematic absences and successful solution and refinement of the structure, the space group was determined to be $Pna2_1$ (No. 33). Single-crystal data were collected on a Bruker Smart CCD diffractometer. The Flack parameter was refined to determine the correct orientation of the crystal. All non-hydrogen atoms were refined using anisotropic thermal parameters. Hydrogen atoms were placed in idealized positions. Atomic coordinates for all atoms other than carbon and hydrogen are listed in Table 2.

$Zn(py)_4Cr_2O_7$. Based on systematic absences and successful solution and refinement of the structure, the space group was determined to be $Pna2_1$ (No. 33). Single-crystal data were collected on a Bruker Smart CCD diffractometer. The Flack parameter was refined to determine the correct orientation of the structure within the crystal. All non-hydrogen positions were refined using anisotropic thermal parameters. Hydrogen atoms were placed in idealized positions. Selected atomic coordinates are listed in Table 3.

Table 3. Selected Atomic Coordinates for $Zn(py)_4Cr_2O_7$

atom	site	x	y	z	B_{eq}[a]	occ
Zn	4a	0.20430(2)	0.74537(3)	0.7727	2.042(9)	1
Cr(1)	4a	0.19310(5)	0.57094(4)	0.4924(1)	2.23(2)	1
Cr(2)	4a	0.29330(4)	0.40129(4)	0.5883(1)	2.78(2)	1
O(1)	4a	0.2119(2)	0.6468(2)	0.6145(4)	2.75(8)	1
O(2)	4a	0.0987(2)	0.5714(2)	0.4518(4)	5.9(1)	1
O(3)	4a	0.2451(2)	0.5817(2)	0.3447(4)	7.4(1)	1
O(4)	4a	0.2103(2)	0.4720(2)	0.5831(4)	4.07(9)	1
O(5)	4a	0.3778(2)	0.4476(2)	0.6100(4)	5.1(1)	1
O(6)	4a	0.2946(2)	0.3451(2)	0.4364(3)	2.76(8)	1
O(7)	4a	0.2770(2)	0.3411(2)	0.7303(3)	4.6(1)	1
N(1)	4a	0.2940(2)	0.6792(2)	0.9000(4)	2.09(9)	1
N(2)	4a	0.1086(2)	0.8080(2)	0.6509(4)	2.3(1)	1
N(3)	4a	0.1112(2)	0.6815(2)	0.8982(4)	2.1(1)	1
N(4)	4a	0.2910(2)	0.8144(2)	0.6426(4)	2.5(1)	1

[a] $B_{eq} = (8/3)\pi^2U_{11}(aa^*)^2 + U_{22}(bb^*)^2 + U_{33}(cc^*)^2 + 2U_{12}(aa^*bb^*)\cos\gamma + 2U_{13}(aa^*cc^*)\cos\beta + 2U_{23}(bb^*cc^*)\cos\alpha$.

Table 4. Selected Atomic Coordinates for $Cd(py)_4Cr_2O_7$

atom	site	x	y	z	B_{eq}[a]	occ
Cd	4c	0.25	0.75	0.5	3.932(7)	1
Cr	8f	0.7481(3)	0.47895(4)	0.44529(3)	4.56(1)	1
O(1)	8f	0.1518(1)	0.5857(2)	0.4722(1)	5.96(6)	1
O(2)	8f	0.0283(3)	0.4553(3)	0.5319(3)	5.9(1)	1/2
O(3)	8f	0.0363(7)	0.461(1)	0.3480(8)	15.5(5)	1/2
O(4)	8f	0.1495(3)	0.3575(4)	0.4580(4)	7.1(2)	1/2
O(5)	8f	0.0001(6)	0.489(1)	0.3420(8)	9.5(2)	1/2
O(6)	8f	0.0984(4)	0.3615(4)	0.4847(5)	11.4(2)	1/2
N(1)	8f	0.2597(1)	0.7340(2)	0.3548(1)	4.03(6)	1
N(2)	8f	0.1176(1)	0.8766(2)	0.4394(1)	4.15(7)	1

[a] $B_{eq} = (8/3)\pi^2U_{11}(aa^*)^2 + U_{22}(bb^*)^2 + U_{33}(cc^*)^2 + 2U_{12}(aa^*bb^*)\cos\gamma + 2U_{13}(aa^*cc^*)\cos\beta + 2U_{23}(bb^*cc^*)\cos\alpha$.

$Cd(py)_4Cr_2O_7$. Based on systematic absences and successful solution and refinement of the structure, the space group was determined to be $C2/c$ (No. 15). Single-crystal data were collected on a Bruker Smart CCD diffractometer. Disorder in the $[Cr_2O_7]^{2-}$ anion results in half-occupancy of the O(2)−O(6) sites. All non-hydrogen positions were refined using anisotropic thermal parameters. Hydrogen atoms were placed in idealized positions. Selected atomic coordinates are listed in Table 4.

Infrared Measurements. Mid-infrared (400−4000 cm^{-1}) spectra were collected using a Bio-Rad FTS-60 FTIR spectrometer operating at a resolution of 2 cm^{-1}.

IR data for $Cu(py)_4Cr_2O_7$, KBr: ν(py) = 1604, 639 cm^{-1}; ν(Cr−O) = 950, 929 cm^{-1}. IR data for $Cd(py)_4Cr_2O_7$, KBr: ν(py) = 1600, 649 cm^{-1}; ν(Cr−O) = 950, 932 cm^{-1}. IR data for $Zn(py)_4Cr_2O_7$, KBr: ν(py) = 1606, 640 cm^{-1}; ν(Cr−O) = 954, 931 cm^{-1}. The infrared bands for the dichromate anion are in good agreement with those reported for $K_2Cr_2O_7$.[18]

Susceptibility. The temperature dependence of the magnetic susceptibility for powdered single crystals of $Cu(py)_4Cr_2O_7$ was determined

(15) *TEXSAN: Crystal Structure Analysis Package*; Molecular Structure Corp.: The Woodlands, TX, 1985 and 1992.
(16) (a) Sheldrick, G. M. SHELXS86. In *Crystallographic Computing 3*; Sheldrick, G. M., Kruger, C., Goddard, R., Eds.; Oxford University Press: Oxford, U.K., 1985; p 175. (b) Altomare, A.; Cascarano, M.; Giacovazzo, C.; Guagliardi, A. *J. Appl. Crystallogr.* **1993,** *26*, 343.
(17) Beurskens, P. T.; Admiraal, G.; Beurskens, G.; Bosman, W. P.; de Gelder, R.; Israel, R.; Smits, J. M. M. DIRDIF-94 program system. Technical Report of the Crystallography Laboratory, University of Nijmegen: Nijmegen, The Netherlands, 1994.
(18) Bates, J. B.; Toth, L. M.; Quist, A. S.; Boyd, G. E. *Spectrochim. Acta* **1973**, *29A*, 1585.

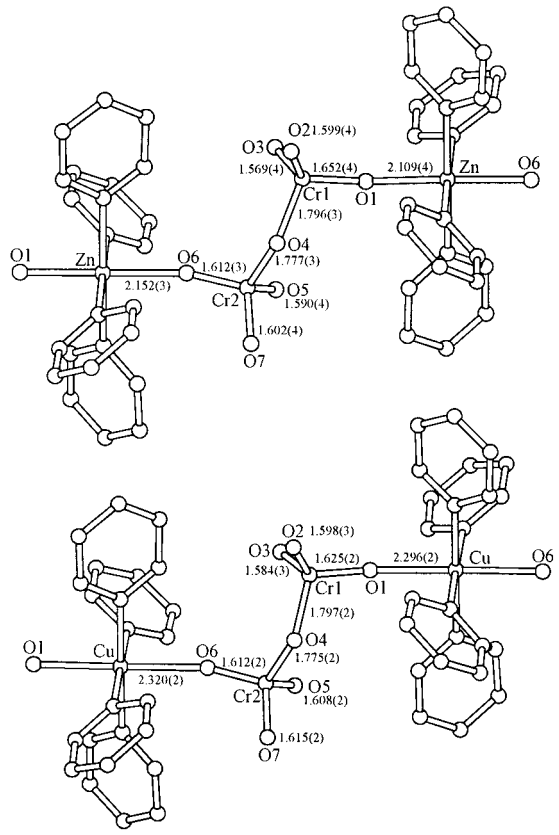

Figure 1. $Cu(py)_4Cr_2O_7$ and $Zn(py)_4Cr_2O_7$ with selected bond lengths included (Å).

with a dc superconductivity quantum interference device (SQUID) magnetometer from Quantum Design. After the powder was zero-field-cooled to 5 K, a 1 kG field was applied and the magnetic moment was registered. The magnetic moment values were calculated from the susceptibility data using the Curie−Weiss law.

Nonlinear Optical Measurements. Powder SHG measurements were performed on a modified Kurtz-NLO[19,20] system using 1064 nm light. A Continuum Minilite II laser, operating at 15 Hz (3 mJ average energy), was used for all measurements. Ungraded SiO_2, $Cu(py)_4Cr_2O_7$, $Cd(py)_4Cr_2O_7$, and $Zn(py)_4Cr_2O_7$ were placed in separate capillary tubes. The SHG, i.e., 532 nm green light, radiation was collected in reflection and detected by a photomultiplier tube (Oriel Instruments). In order to detect only the SHG light, a 532 nm narrow band-pass interference filter was attached to the tube. A digital oscilloscope (Tektronix TDS 3032) was used to view the SHG signal.

Results

$Cu(py)_4Cr_2O_7$ and $Zn(py)_4Cr_2O_7$. $Cu(py)_4Cr_2O_7$ and $Zn(py)_4Cr_2O_7$ are isostructural. See Figure 1. Bond lengths and angles for $Cu(py)_4Cr_2O_7$, $Zn(py)_4Cr_2O_7$, and $Cd(py)_4Cr_2O_7$ are listed in Table 5. The nonbridging Cr−O distances in $Cu(py)_4Cr_2O_7$ and $Zn(py)_4Cr_2O_7$ are 1.602(4), 1.590(4), 1.569(4), and 1.599(4) Å, whereas the bridging Cr−O distances are 1.612(3), 1.777(3), 1.796(3), and 1.652(4) Å. These tetrahedra mimic the distorted phosphate tetrahedra in the ferroelectric KH_2PO_4 where the phosphorous ion is distorted toward an edge resulting in two long (1.56 Å) and two short (1.53 Å) bonds. The Cr^{VI} form nearly regular tetrahedra with an average O−Cr−O bond angle = 109.4° for each $[Cr_2O_7]^{2-}$. The Cr−O−Cr bond angle deviates significantly from 180°, 134.0(2)° and 129.7(5)° for $Zn(py)_4Cr_2O_7$ and $Cu(py)_4Cr_2O_7$, respectively. The bond lengths and angles of the dichromate anion, in $Cu(py)_4Cr_2O_7$ and $Zn(py)_4Cr_2O_7$, are in good agreement with $Na_2Cr_2O_7$.[21] O(2), O(3), O(5), and O(7) exhibit large B_{eq}'s with respect to the other atoms, see Tables 2 and 3. Unlike the O(1), O(4), and O(6) which are two-coordinate, these oxide ligands are only bound to one chromium center. The thermal motion of these ligands can be observed in their elongated thermal parameters.

Table 5. Selected Bond Lengths (Å) and Angles (deg) for $M(py)_4Cr_2O_7$ (M = Cu, Zn, Cd)

$Cu(py)_4Cr_2O_7$			
Bond Lengths			
Cr(1)−O(1)	1.625(2)	Cr(2)−O(5)	1.608(2)
Cr(1)−O(2)	1.598(3)	Cr(2)−O(6)	1.612(2)
Cr(1)−O(3)	1.584(3)	Cr(2)−O(7)	1.615(2)
Cr(1)−O(4)	1.797(2)	Cu−O(1)	2.296(2)
Cr(2)−O(4)	1.775(2)	Cu−O(6)	2.320(2)
Bond Angles			
O(1)−Cu−O(6)	175.92(9)	O(4)−Cr(2)−O(6)	110.1(1)
O(1)−Cr(1)−O(4)	108.3(1)	Cu−O(1)−Cr(1)	164.7(1)
Cr(1)−O(4)−Cr(2)	129.7(1)	Cu−O(6)−Cr(2)	165.7(1)
$Zn(py)_4Cr_2O_7$			
Bond Lengths			
Cr(1)−O(1)	1.652(4)	Cr(2)−O(5)	1.590(4)
Cr(1)−O(2)	1.599(4)	Cr(2)−O(6)	1.612(3)
Cr(1)−O(3)	1.569(4)	Cr(2)−O(7)	1.602(4)
Cr(1)−O(4)	1.796(3)	Zn−O(1)	2.109(4)
Cr(2)−O(4)	1.777(3)	Zn−O(6)	2.152(3)
Bond Angles			
O(1)−Zn−O(6)	176.1(1)	O(4)−Cr(2)−O(6)	110.1(2)
O(1)−Cr(1)−O(4)	109.2(2)	Zn−O(1)−Cr(1)	165.8(2)
Cr(1)−O(4)−Cr(2)	134.0(2)	Zn−O(6)−Cr(2)	166.0(2)
$Cd(py)_4Cr_2O_7$			
Bond Lengths			
Cr−O(1)	1.604(2)	Cr−O(5)	1.63(1)
Cr−O(2)	1.748(4)	Cr−O(6)	1.444(6)
Cr−O(3)	1.838(5)	Cd−O(1)	2.290(2)
Cr−O(4)	1.720(6)		
Bond Angles			
O(1)−Cr−O(2)	102.3(2)	O(1)−Cr−O(2)	109.8(2)
O(1)−Cr−O(3)	111.6(9)	O(1)−Cr−O(4)	100.8(2)
O(1)−Cr−O(6)	121.2(3)	O(1)−Cr−O(5)	112.9(6)
O(2)−Cr−O(3)	102.2(6)	O(2)−Cr−O(4)	101.5(3)
O(2)−Cr−O(6)	111.9(4)	O(2)−Cr−O(5)	118.6(6)
O(3)−Cr−O(6)	106.2(9)	O(4)−Cr−O(5)	111.2(5)

The cations consist of a central Cu^{2+} or Zn^{2+} cation with four pyridine rings in a square planar arrangement. The axially distorted Jahn−Teller Cu^{2+} cations contain four "short" equatorial bonds to pyridine (2.039(3), 2.030(3), 2.029(2), 2.025(2) Å) and two "long" axial bonds to oxygen (2.296(2) and 2.320(2) Å). The spherical Zn^{2+} cation, as expected, bonds to four pyridine rings through lengths of 2.138(4), 2.157(5), 2.151(4), and 2.141(4) Å, while the Zn−O bond lengths are 2.109(4) and 2.152(3) Å.

Neutral nonintersecting one-dimensional chains of $M(py)_4Cr_2O_7$ (M = Cu, Zn) are formed. The $[M(py)_4]^{2+}$ cations are bound to the dichromate anions through trans coordination sites. The dichromate anions are rotated 90° with respect to one another within each chain as shown in Figure 2. Layers (0 1 1) of parallel chains are rotated 90° every *a*/2 as shown in Figure 3.

The molar moment showed $Cu(py)_4Cr_2O_7$ to be a Curie paramagnet with a $\mu_{eff} = 1.73\ \mu_B$, in good agreement with isolated Cu^{2+} (d^9) cations. The Weiss constant is low, on the order of 0.1°, consistent with the shortest Cu−Cu distance of 8.86 Å.

(19) Kurtz, S. K.; Perry, T. T. *J. App. Phys.* **1968**, *39*, 3798.
(20) Dougherty, J. P.; Kurtz, S. K. *J. Appl. Crystallogr.* **1976**, *9*, 145.
(21) Panagiotopoulos, N. P.; Brown, I. D. *Acta Crystallogr., Sect B.* **1972**, *28*, 1352.

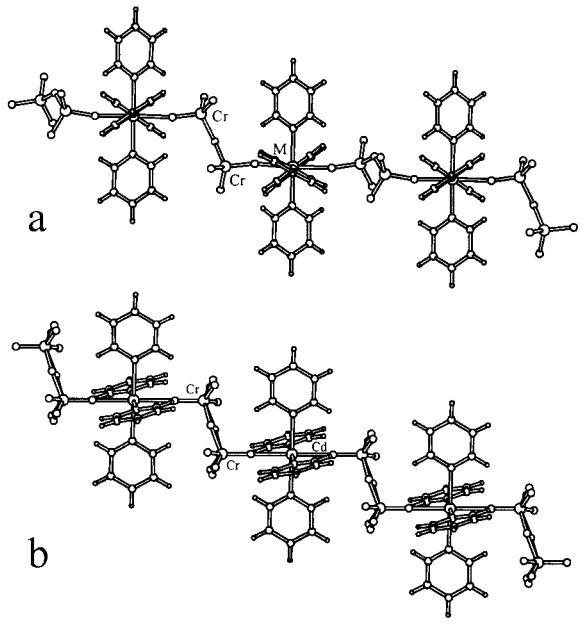

Figure 2. (a) One-dimensional chain of $M(py)_4Cr_2O_7$ (M = Cu, Zn) showing the 90° rotation in the $[Cr_2O_7]^{2-}$ anion. (b) One-dimensional chain of $Cd(py)_4Cr_2O_7$ showing no rotation in the $[Cr_2O_7]^{2-}$ anion.

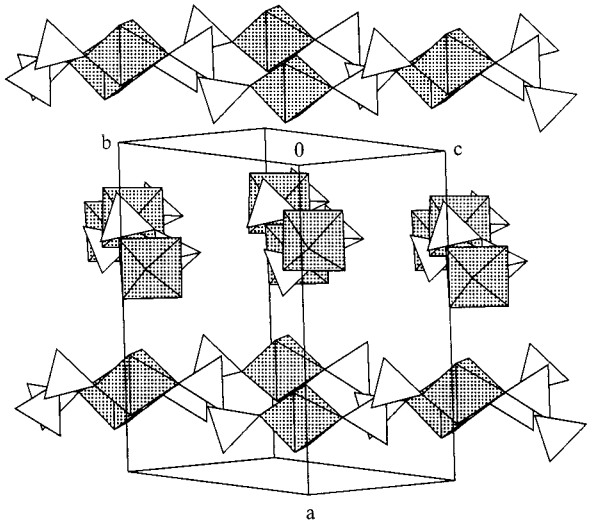

Figure 3. Packing diagram of $M(py)_4Cr_2O_7$ (M = Cu, Zn). Shaded octahedra represent $[M(py)_4]^{2+}$, and unshaded corner-shared tetrahedra represent $[Cr_2O_7]^{2-}$. Pyridine rings have been removed for clarity.

$Cd(py)_4Cr_2O_7$. Crystallographic disorder in the $[Cr_2O_7]^{2-}$ anion results in the superimposition of two orientations upon one another as shown in Figure 4. The ligands O(1) and O(2) are common to both orientations, while the remaining two ligands in each tetrahedron consist of either O(3) and O(6), or O(4) and O(5). O(3) and O(6) exhibit abnormally large B_{eq}'s with respect to the other atoms, suggesting an unequal population of the two disorder orientations. However, O(2) is constrained to occupy two sites equally, eliminating in this model and space group the possibility of O(3) and O(6) having less than $^1/_2$ occupancy.

The average Cd−N bond length is 2.347(5) Å, and the Cd−O(1) bond is 2.290(2) Å. The increase in M−N and M−O bond lengths for M = Cd compared to M = Zn reflects an increase in ionic radii between six-coordinate Zn^{2+} and Cd^{2+}, 0.74 and 0.95 Å, respectively.[21]

The structural motif of neutral one-dimensional chains composed of alternating $[Cd(py)_4]^{2+}$ cations and $[Cr_2O_7]^{2-}$ anions is observed in $Cd(py)_4Cr_2O_7$ as shown in Figure 5. The $[Cr_2O_7]^{2-}$ anions adopt the same orientation within each chain in $Cd(py)_4Cr_2O_7$, differing from the 90° rotation of the anions in $M'(py)_4Cr_2O_7$ (M′ = Cu, Zn) as shown in Figure 2.

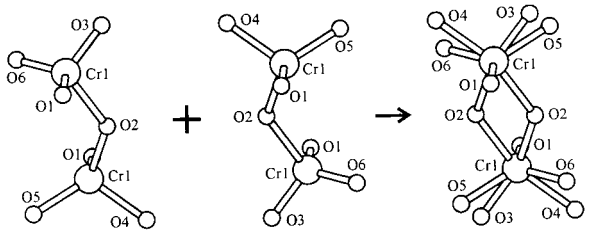

Figure 4. Disorder mechanism for the corner-shared $[Cr_2O_7]^{2-}$ tetrahedra in $Cd(py)_4Cr_2O_7$. The superimposition of the two orientations results in the final model.

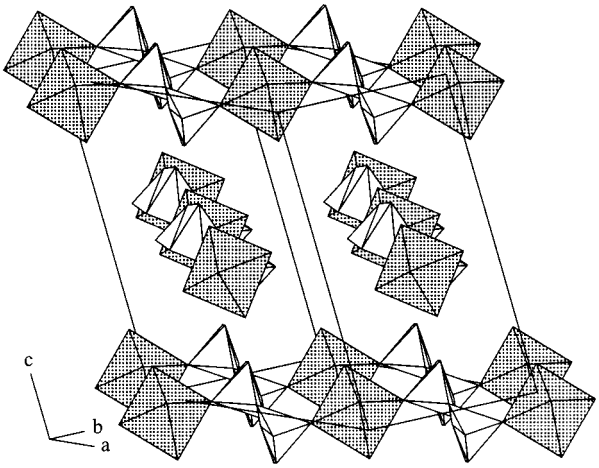

Figure 5. Packing diagram of $Cd(py)_4Cr_2O_7$. Shaded octahedra represent $[Cd(py)_4]^{2+}$, and unshaded polyhedra represent $[Cr_2O_7]^{2-}$. Pyridine rings have been removed for clarity.

Nonlinear Optical Measurements. The second-order NLO properties of $Cu(py)_4Cr_2O_7$, $Zn(py)_4Cr_2O_7$, and $Cd(py)_4Cr_2O_7$ were measured using the Kurtz powder technique. $Zn(py)_4Cr_2O_7$ exhibited a signal comparable to α-quartz under the same conditions. No signal was observed for $Cu(py)_4Cr_2O_7$ owing to absorption of the incident beam. No signal was observed for $Cd(py)_4Cr_2O_7$ because this compound crystallizes in a centrosymmetric space group.

Discussion

The presence of a nonspherical Jahn−Teller active cation, Cu^{2+}, affects the unit cell dimensions of $M(py)_4Cr_2O_7$ (M = Cu, Zn) with respect to Zn^{2+}. The elongation of the Jahn−Teller axis in $Cu(py)_4Cr_2O_7$ results in an increase in the unit cell parameters *b* and *c*, 16.324(3) and 8.857(2) Å in $Cu(py)_4Cr_2O_7$ versus 16.005(1) and 8.8130(5) Å in $Zn(py)_4Cr_2O_7$ because the one-dimensional chains run in the direction of the *b* and *c* axes. The unit cell parameter *a*, which runs perpendicular to the one-dimensional chains, is longer in the Zn analogue than in the Cu analogue because the average Zn−N bond distance, 2.14(1) Å, is greater than that of the Cu−N bond, 2.04(1) Å.

The structures of $M(py)_4Cr_2O_7$ (M = Cu, Zn) and KTP[7] share several striking similarities. KTP consists of helical $TiO_{4/2}O_{2/2}$ chains linked by phosphate tetrahedra. Each layer, composed of parallel chains, is rotated 90° every *a*/2. The $M(py)_4Cr_2O_7$ (M = Cu, Zn) chains also pack in this fashion. Figure 6 shows the common structural themes in $M(py)_4Cr_2O_7$ (M = Cu, Zn) and KTP. The $TiO_{4/2}O_{2/2}$ chains in KTP contain two types of $TiO_{4/2}O_{2/2}$ octahedra, either a cis or trans orientation of the

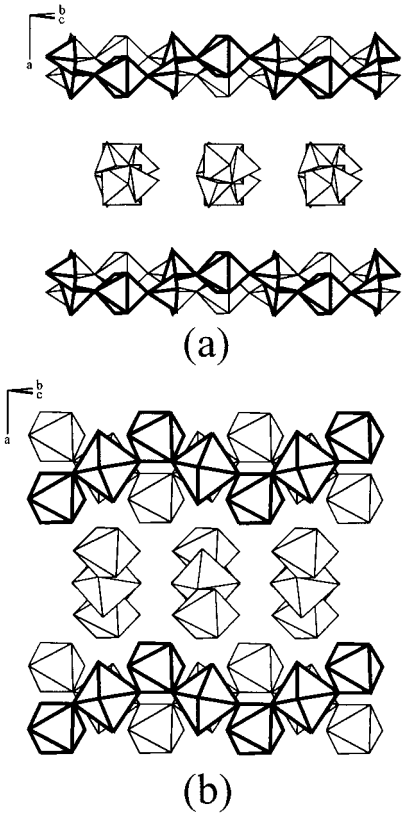

Figure 6. Packing diagram of (a) $M(py)_4Cr_2O_7$ (M = Cu, Zn) and (b) KTP. Pyridine rings from part a and phosphate tetrahedra and K^+ ions from part b have been removed for clarity.

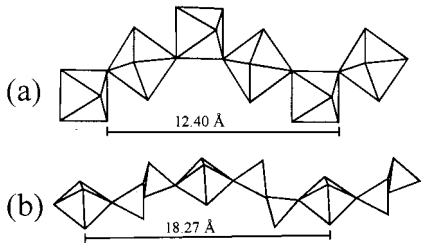

Figure 7. Helical chains of (a) $TiO_{4/2}O_{2/2}$ and (b) $M(py)_4Cr_2O_7$ (M = Cu, Zn).

bridging oxygens with respect to one another. The cis and trans coordinated $TiO_{4/2}O_{2/2}$ octahedra are replaced by $[M(py)_4]^{2+}$ (M = Cu, Zn) and $[Cr_2O_7]^{2-}$ respectively in $M(py)_4Cr_2O_7$ (M = Cu, Zn). The $TiO_{4/2}O_{2/2}$ and $M(py)_4Cr_2O_7$ (M = Cu, Zn) chains are shown in Figure 7.

With the similarities some differences also exist. The length of each rotation in the $M(py)_4Cr_2O_7$ (M = Cu, Zn) chains, 18.57 and 18.27 Å, respectively, is longer than the corresponding $TiO_{4/2}O_{2/2}$ rotation, 12.40 Å. Also, in $M(py)_4Cr_2O_7$ (M = Cu, Zn) the chains are not covalently bound to one another, van der Waals forces support the structure, while in KTP phosphate tetrahedra connect the nonintersecting $TiO_{4/2}O_{2/2}$ chains.

Kurtz powder experiments on $Zn(py)_4Cr_2O_7$ demonstrate the second-order NLO properties inherent to the polar space group $Pna2_1$. No second-order signal was observed from $Cu(py)_4Cr_2O_7$ owing to absorption of the incident radiation by the powder. $Zn(py)_4Cr_2O_7$, however, suffers from no such problems and the SHG signal at 532 nm was measured. $Cd(py)_4Cr_2O_7$ crystallizes in the space group $C2/c$ (No. 15). This space group is indistinguishable from Cc (No. 9) based on systematic absences. If $Cd(py)_4Cr_2O_7$ crystallized in Cc, no disorder in the $[Cr_2O_7]^{2-}$ anion would be expected and the compound would exhibit second-order NLO properties. The centrosymmetric disorder model is consistent with the null result from SHG test. If the compound crystallizes in Cc, the noncentrosymmetric space group, a positive second-order NLO result is expected because no absorption was encountered in $Zn(py)_4Cr_2O_7$, a compound with similar optical properties.

Conclusion

The combination of the two molecular ions, $[Cr_2O_7]^{2-}$ and $[M(py)_4]^{2+}$ (M = Cd, Cu, Zn), and subsequent crystallization at 150 °C has resulted in three new transition metal oxides, two of which crystallize in the polar space group $Pna2_1$. The noncentrosymmetric phases $M'(py)_4Cr_2O_7$ (M′ = Cu, Zn) consist of one-dimensional chains that are quite similar to the $TiO_{4/2}O_{2/2}$ helical chains in KTP.[22−25] The use of corner-shared tetrahedral anions to enforce acentricity upon a metal oxide chain is a novel strategy for the discovery of new noncentrosymmetric, polar materials.

Acknowledgment. The authors gratefully acknowledge support from the National Science Foundation, Solid State Chemistry (Award No. DMR-9727516), and made use of the Central Facilities supported by the MRSEC program, National Science Foundation, at the Materials Research Center of Northwestern University (Award No. DMR-0076097).

Supporting Information Available: Magnetic susceptibility plots and tables and three thermal ellipsoid plots. Three X-ray crystallographic information files in CIF format. This material is available free of charge via the Internet at http://pubs.acs.org.

IC000953Y

(22) Jacco, J. C.; Loiacono, G. M.; Jaso, M.; Mizell, G.; Greenberg, B. *J. Cryst. Growth* **1984,** *70*, 484.
(23) Ballman, A. A.; Brown, H.; Olson, D. H.; Rice, C. E. *J. Cryst. Growth* **1986,** *75*, 390.
(24) Belt, R. F.; Gashurov, G. *SPIE Int. Soc. Opt. Eng.* **1988**, *968*, 100.
(25) Laudise, R. A.; Sunder, W. A.; Belt, R. F.; Gashurov, G. *J. Cryst. Growth* **1990,** *102*, 427.